Published in final edited form as:
Bioconjug Chem. 2011 October 19; 22(10): 1983–1993. doi:10.1021/bc200173e.

Novel anticancer polymeric conjugates of activated nucleoside analogs

Thulani H. Senanayake, **Galya Warren**, and **Serguei V. Vinogradov***
Center for Drug Delivery and Nanomedicine and Department of Pharmaceutical Sciences, College of Pharmacy, University of Nebraska Medical Center, Omaha, United States

Abstract

Inherent or therapy-induced drug resistance is a major clinical setback in cancer treatment. The extensive usage of cytotoxic nucleobases and nucleoside analogs in chemotherapy also results in the development of specific mechanisms of drug resistance; such as nucleoside transport or activation deficiencies. These drugs are prodrugs; and being converted into the active mono-, di- and triphosphates inside cancer cells following administration, they affect nucleic acid synthesis, nucleotide metabolism, or sensitivity to apoptosis. Previously, we have actively promoted the idea that the nanodelivery of active nucleotide species, e.g. 5′-triphosphates of nucleoside analogs, can enhance drug efficacy and reduce nonspecific toxicity. In this study we report the development of a novel type of drug nanoformulations, polymeric conjugates of nucleoside analogs, which are capable of the efficient transport and sustained release of phosphorylated drugs. These drug conjugates have been synthesized, starting from cholesterol-modified mucoadhesive polyvinyl alcohol or biodegradable dextrin, by covalent attachment of nucleoside analogs through a tetraphosphate linker. Association of cholesterol moieties in aqueous media resulted in intramolecular polymer folding and the formation of small nanogel particles containing 0.5 mmol/g of a 5′-phosphorylated nucleoside analog, e.g. 5-fluoro-2′-deoxyuridine (floxuridine, FdU), an active metabolite of anticancer drug 5-fluorouracyl (5-FU). The polymeric conjugates demonstrated rapid enzymatic release of floxuridine 5′-phosphate and much slower drug release under hydrolytic conditions (pH 1.0–7.4). Among the panel of cancer cell lines, all studied polymeric FdU-conjugates demonstrated an up to 50 times increased cytotoxicity in human prostate cancer PC-3, breast cancer MCF-7 and MDA-MB-231 cells, and more than 100 times higher efficacy against cytarabine-resistant human T-lymphoma (CEM/araC/8) and gemcitabine-resistant follicular lymphoma (RL7/G) cells as compared to free drugs. In the initial *in vivo* screening, both PC-3 and RL7/G subcutaneous tumor xenograft models showed enhanced sensitivity to sustained drug release from polymeric FdU-conjugate after peritumoral injections and significant tumor growth inhibition. All these data demonstrate a remarkable clinical potential of novel polymeric conjugates of phosphorylated nucleoside analogs, especially as new therapeutic agents against drug-resistant tumors.

Introduction

Despite several decades of research and drug development, progress in the clinical struggle against cancer has been only moderate. Development of resistance by cancer cells to chemotherapeutic agents has currently become a major clinical problem, limiting the effectiveness of the treatment of hematological malignancies as well as solid tumors.

*Correspondent author. 986025 Nebraska Medical Center, Omaha, NE 68198-6025; Phone: (402) 559-9362; Fax: (402) 559-9543; vinograd@unmc.edu.

Supporting information available: Analytical characteristics (^{1}H-NMR and IR spectra, Figures S1–S3) of synthesized products. This material is available free of charge via the Internet at http://pubs.acs.org.

Multiple studies have helped to identify many mechanisms of drug resistance, but in general terms they can all be reduced to the prevention of a drug from entering cells, deactivation of drug molecules, or the enhanced resistance of cancer cells to apoptosis. The first group includes deficiencies in membrane nucleoside transporters, or the overexpression of ATP-dependent drug efflux transporters like P-glycoprotein (MDR) and other membrane proteins (MRP) responsible for drug efflux. In the second group, the drug metabolism/degradation and reduced levels of enzymatic drug activation should be mentioned. In the third group, the induction of anti-apoptotic mechanisms, as well as the suppression of pro-apoptotic pathways plays important roles in drug resistance[1].

Cytotoxic nucleoside analogs belong to the important class of anticancer drugs, which are currently used as the first-line treatment of hematological malignancies and certain solid tumors[2]. These drugs act as antimetabolites by interfering with nucleic acid synthesis and enzymes of the nucleotide metabolism. The clinical efficacy of these drugs depends on higher metabolic activity and drug activation in rapidly proliferating cancer cells compared to normal cells. Activation of therapeutic nucleoside analogs occurs through the *de novo* synthesis of 5′-mono-, di- and triphosphate derivatives, which interfere with the cellular pool of natural nucleosides. Nucleoside analogs require participation of specialized nucleoside transporter proteins such as hENT1, hENT2, hCNT1 in order to accumulate in the cells. The integral drug uptake depends on the proper balance of the nucleoside transporters and drug efflux proteins presented on cellular membrane. Therefore, the drug accumulation is substantially reduced when the expression of such nucleoside transporters is deficient[3,4], or the activity of drug efflux transporter proteins is elevated[5,6]. After entering cells, nucleoside analogs undergo phosphorylation into 5′-monophosphates with deoxycytidine kinase (dCK) or thymidine kinase (TK), a rate-limiting step in the intracellular activation of nucleosides, and are subsequently converted into active 5′-diphosphates and 5′-triphosphates by other nucleoside kinases[3]. The efficacy of nucleoside analogs may further be limited by additional factors such as metabolic deamination and intracellular dephosphorylation[7,8].

In order to increase tumor accumulation of nucleoside analogs, various prodrug and drug delivery approaches have been developed; for example, the application of lipophilic nucleoside derivatives with an enhanced cellular membrane affinity. Many prodrugs with degradable lipophilic masking groups demonstrate the enhanced cell membrane permeability[9]. Early phase clinical trials have shown some improvements in the treatment of hematological malignancies, but these prodrugs were not effective in the treatment of solid tumors[10]. Moreover, lipophilic prodrugs have a reduced half-life in circulation due to the fast accumulation in liver. Various nanocarriers such as liposomes, biodegradable nanoparticles, polymeric micelles and nanocapsules have been extensively for tumor delivery of chemotherapeutic drugs[11]. Many of these nanocarriers demonstrated advanced features, but have also shown serious shortcomings limiting their clinical usefulness. For example, liposomal formulations were unable to achieve effective drug concentration inside tumors because many anticancer drugs (cytarabine, 5-FU, etc) diffused rapidly through the liposome bilayer[12].

Recently, we introduced an alternative tumor treatment strategy using formulation and nanodelivery of activated drugs, nucleoside 5′-triphosphates, encapsulated in cationic nanogels[17]. Previously, several laboratories have attempted to achieve *in vivo* delivery of bioactive 5′-triphosphates of nucleoside analog through encapsulation in liposomes[13,14], nanoparticles[15], or red blood cells[16]. Evidently, the success of this strategy depends on the advantages of nanoformulations in drug protection in biological milieu, controlled drug release, and the specific tumor targeting. Nanogel carriers have dramatically improved the delivery of activated phosphorylated nucleoside analogs into cancer cells and tumor growth inhibition effect[18,19]. However, the non-covalent nature of the encapsulation of anionic 5′-

triphosphates in cationic nanogels was the reason of relatively fast drug release kinetics. Here, we report synthesis of novel types of drug-loaded nanogels, containing polymer network with covalently linked phosphorylated nucleoside analogs, which are capable of sustained drug release and structurally different from the previously studied polymeric nanogels. Covalent drug attachment is an important factor of the controlled drug release, because it allows using specific chemistries. Various hydrolytically or enzymatically-sensitive linkers such as peptides, carboxylates, etc have been previously evaluated with polymeric drug delivery systems[20–22]. In this study, drug conjugates were synthesized by the attachment of nucleoside analogs through a biodegradable tetraphosphate linker starting from amphiphilic polymers such as cholesterol-modified polyvinyl alcohol (PVA) or dextrin (DEX). The linker has strong advantage over other linkers, because the polymeric drug conjugates are able to release nucleoside analogs in active phosphorylated form in the result of its hydrolytic or enzymatic degradation, eventually showing an enhanced tumor growth inhibition efficacy against normal and drug-resistant cancer cells. These drug-containing polymer conjugates can form stable nanogels with a small hydrodynamic diameter after ultrasonication in aqueous media as demonstrated in Figure 1. Selection of biodegradable or mucoadhesive biocompatible polymers for preparation of polymeric conjugates might also reduce toxicity of chemotherapy and open potentials for oral administration of these nanoformulations.

Materials and Methods

Materials

Most reagents, solvents, and polymers were purchased from Sigma Aldrich (St. Louis, MO) and Alfa Aesar (Wardhill, MA) with the highest available purity and used without purification unless otherwise stated. Thymidine, 3-[4,5-dimethylthiazol-2-yl]-2,5-diphenyltetrazolium bromide (MTT) and snake venom phosphodiesterase 1, type VI, from Carotalus adamanteus were purchased from Sigma (St. Louis, MO). Nucleoside analogs: 5-fluro-2′-deoxyuridine (Floxuridine, FdU) was from SynQuest Laboratories (Alachua, FL), 2, 2′-difluorocytidine (dFdC, Gemcitabine) was from Beta Pharma, Inc (Branford, CT), and arabinosylcytosine (araC, Cytarabine) was from 3B Medical Systems, Inc (Libertyville, IL). Centrifuge filter devices (MWCO 5,000 Da) were purchased from Millipore (Bedford, MA).

All NMR spectra were recorded using a 500 MHz Varian NMR- spectrometer. All chemical shift values are given in parts per million (ppm) and are referenced to a signal from $(CH_3)_4Si$ (0 ppm) for ^1H, DMSO-d_6 (39.7 ppm) for ^{13}C, and 85% phosphoric acid (0 ppm) for ^{31}P spectra at 25°C. Hydrodynamic diameter, polydispersity, and zeta-potential of nanogels and polymeric conjugates were measured using a dynamic light scattering instrument, the Zetasizer Nano-ZS90 (Malvern Instruments, Southborough, MA) at 25°C. Monodisperse polystyrene dispersions were used as standards. UV absorbance of samples was measured by Biophotometer (Eppendorf, Hamburg, Germany). IR spectra were recorded using a Nicolet IR-200 FT-IR spectrometer (Thermo Scientific, Waltham, MA).

Cells

Human breast carcinoma MCF-7, human hepatocellular carcinoma HepG2, and human prostate adenocarcinoma PC-3 cells were obtained from ATCC (Rockville, MD). These cells were maintained in Dulbecco's Modified Eagle Medium (DMEM) supplemented with 10% fetal bovine serum (FBS), 1% L-glutamine and 2% penicillin-streptomycin at 37°C in a humidified atmosphere containing 5% CO_2. Human breast carcinoma MDA-MB-231 cell line was a gift from Dr. R. Singh (UNMC). These cells were maintained in DMEM: Nutrient mixture F-12 (DMEM/F12) with similar supplements and serum as above. Gemcitabine-resistant human follicular lymphoma RL7/G cell line, which is characterized by a reduced

level of dCK enzyme[23], was a gift from Dr. F. Bontemps (De Duve Institute, Bruxelles, Belgium). They were grown in the presence of 2 μM gemcitabine. Nucleoside transport-deficient cytarabine-resistant human leukemic lymphoblast CEM/araC/8 cell line[24] was obtained from Dr. C. Galmarini (UFR Lyon-Sud, Oullins, France). The cells were grown in the presence of 0.5 μM cytarabine (araC). Both drug-resistant cell lines were grown in RPMI medium supplemented with 10% fetal bovine serum (FBS), 1% L-glutamine, and 2% penicillin-streptomycin at 37°C in a humidified atmosphere containing 5% CO_2.

Synthesis of cholesterol conjugates

PVA was grafted with cholesterol moieties according to the procedures described below. Briefly, 2.1 g of PVA (M.w. 13 kDa) was dried over phosphorus pentoxide *in vacuo* and dissolved in 50 mL of anhydrous DMSO at 70 °C. Triethylamine (0.8 mmol) was added to the cooled solution (25°C) followed by 0.3g (0.68 mmol) of cholesteryl chloroformate, and the final solution was stirred overnight at 25°C. The reaction mixture was concentrated *in vacuo* and dialyzed (MWCO 3.5 kDa) against 20% aqueous ethanol three times for 24 hours. The product (CPVA) was isolated after concentration *in vacuo* and freeze-drying with a yield of 80%. In another method, 2.1 g of PVA (M.w. 13 kDa) was dissolved in 50 mL of anhydrous N-methyl pyrrolidone at 70°C, then 0.3g (0.68 mmol) of cholesteryl chloroformate was added, and the mixture was stirred for 4h at 70°C. The substituted CPVA was precipitated in diethyl ether (0.5L) and dried *in vacuo*; the light yellow precipitate was obtained with a yield of 70%. ^{1}H-NMR: 0.63 (s, 18H), 0.83 (m, 36H), 0.88 (m, 18H), 0.92 (s, 18H), 1.11–1.95(m, 764H), 3.84–3.90(m, 295H), 4.31(brs, OH), 4.40(s, 12H), 5.25(s, 6H). Following the same protocol for PVA (M.w. 31 kDa), we obtained CPVA with a yield of 85%. ^{1}H-NMR: 0.65 (s, 18H), 0.83–0.85(dd, J=5.0, 1.6 Hz, 36H), 0.89(d, J=4.8 Hz, 18H), 0.94(s, 18H), 1.07–1.98(m, 1582H), 3.84(m, 704H), 4.35(12H and OH), 5.28(s, 6H). IR: 3264, 2897, 1642, 1409, 1323, 1082, 915, 829.

The dextrin-cholesterol nanogel (CDEX) was synthesized as follows. The water-soluble fraction of dextrin (M.w. 9 kDa) was isolated by dialysis in a SpectraPor membrane tube (MWCO 2 kDa) followed by centrifugation. The supernatant was freeze-dried and used for nanogel synthesis. 1.0 g of the purified dextrin was dried over phosphorus pentoxide *in vacuo* and dissolved in 15 mL of anhydrous DMSO at 70°C. After 0.3g (0.68 mmol) of cholesteryl chloroformate was added, the reaction mixture was stirred for 24h at 25°C, concentrated *in vacuo* and dialyzed (MWCO 3.5 kDa) against 20% aqueous ethanol three times for 24 hours. The product (CDex) was isolated after concentration *in vacuo* and freeze-drying with a yield of 76%. ^{1}H-NMR: 0.65 (s, 18H), 0.83–0.85(dd, J=5.0, 1.6 Hz, 36H), 0.89–1.51(m, 211H), 3.24–3.64(m, 333H), 4.28–5.10 (m, 122H), 5.23(s, 6H), 5.37–5.62(m, 55H).

Synthesis of phosphorylating reagent, $CNEtOP(O)Im_2$

The intermediate product $CNEtOP(O)Cl_2$ was synthesized by dissolving 18.6 mL (30.6 g, 0.2 mol) phosphorus(V) oxychloride and 20.6 mL (14.84 g, 0.147 mol) triethylamine in 40 mL anhydrous tetrahydrofuran (THF) at 0°C. It was treated with 10 mL (10.45 g, 0.147 mol) 2-cyanoethanol in 5mL THF while stirring at 0°C. Stirring was continued for 30 minutes until white precipitate formed. The precipitate was carefully filtered with exclusion of moisture, and the resulting solution was concentrated *in vacuo* and distilled under argon. The product, $CNEtOP(O)Cl_2$ was recovered at 90°C/1 mm with a yield of 60%.

The product, $CNEtOP(O)Im_2$ was synthesized by mixing 2.69 g (0.015 mol) $CNEtOP(O)Cl_2$ and 5.25g (0.037 mol) N-trimethylsilyl-imidazole in 40 mL cold anhydrous toluene. The solutions were then incubated for 2h at room temperature, concentrated *in vacuo* to a half-

volume and placed in a freezer for 2 h at −20 °C. The precipitate of $CNEtOP(O)Im_2$ was recovered after centrifugation with a yield of 70%[25].

Preparation of polymeric drug conjugates

A solution of 3.3 g of dried cholesterol-polymer conjugates in 33 mL DMF was treated with a 2M solution of $CNEtOP(O)Im_2$ in anhydrous DMF (2 mL) for 30 min at 25°C. Then, a 1M solution of tetra-n-butylammonium salt of pyrophosphate (PPi-TBA) in anhydrous DMF (4 mL) was added, and the reaction mixture was incubated for 1 h at 25°C. In a separate flask, floxuridine (FdU, 490 mg, 2 mmol) was treated with a 2M solution of $CNEtOP(O)Im_2$ in anhydrous DMF (1 mL) and allowed to stand for 20 min at 25°C. Both solutions were then mixed and stirred for 40 min at 25°C. The reaction mixture was treated with 1 mL of methanol and left overnight at 4°C. Insoluble material was removed by filtration; the nanogel conjugate was purified three times over 24 h by dialysis (MWCO 3,500 Da) against 20% aqueous ethanol, concentrated *in vacuo* and precipitated as a sodium salt in acetone. FdU content in the nanogel conjugate was measured by UV absorbance (ε_{260} = 7,570). Drug loading: CPVA31, 0.51 μmol/mg; CPVA13, 0.50 μmol/mg; and CDex9, 0.44 μmol/mg.

Particle size and zeta-potential measurements

The hydrodynamic diameter and polydispersity of nanogels and polymeric conjugates were measured by dynamic light scattering (DLS) using a Zetasizer Nano-ZS90 with a 15 mV solid state laser operated at a wavelength of 635 nm. In brief, dry samples were resuspended in filtered de-ionized water, then sonicated for 1 h at 4°C to form a uniform dispersion of nanoparticles and centrifuged for 4 min at 10,000 ×*g*. The size distribution in samples was characterized by polydispersity index. Zeta-potential was calculated based on electrophoretic mobility measurements performed with an electrical field strength of 15–18 V cm^{-1} at 25°C using the instrument software. The data reported in Table 1 represents an average of three measurements.

Enzymatic hydrolysis

Enzymatic stability and drug release from polymeric conjugates was assayed in 50μL reaction mixtures containing: 100 mM Tris-HCl (pH 8.75), 2 mM $MgCl_2$, 0.5 mg of snake venom phosphodiesterase (VPDE) and 0.5 mg nanogel sample (FdU, 0.25 μmol). The reaction mixture was incubated at 37°C and, at appropriate times, 5 μL aliquots were taken out and quenched with 1.5 μL of 1M HCl. Nucleotide content was analyzed by ion-pair HPLC using an Ascentis C18 column (10 μm, 15cm × 4.6mm) at a flow rate of 1 mL/min. The elution was performed with buffer A: 40 mM KH_2PO_4, 0.2% tetrabutylammonium hydroxide, pH 7.0, and buffer B: 30% acetonitrile, 40 mM KH_2PO_4, 0.2% tetrabutylammonium hydroxide, pH 7.0, in a linear gradient mode (100% B in 20 min).

In vitro drug release

In vitro drug release was investigated under different pH values. In short, 18 mg of CPVA31-p_4FdU or CDex9-p_4FdU conjugates was dissolved in 20 ml of PBS solution at pH 7.4, 4.0 and 1.0. These solutions were incubated at 37°C and 0.5 mL-aliquots were taken out every 24 h. The released nucleotides were separated from the rest of the polymeric conjugates by centrifugation at 7,500 rpm for 25 min using an Amicon Ultra-0.5 centrifuge filter device (MWCO 3,000 Da). The pH of the filtrate was adjusted to 7.4 and UV absorbance was measured at 260 nm.

Cytotoxicity studies

Cytotoxicity of the polymeric conjugates was analyzed in different cancer cell lines by a standard MTT assay. Briefly, MCF-7, PC-3, HepG2, and MDA-MB-231 cells were seeded

at a density of 10,000 cells/200 μL growth medium/well in flat-bottom 96-well plates; the corresponding suspensions of RL7/G and CEM/araC/8 cells were placed in round-bottom 96-well plates. Cells were allowed to grow overnight and appropriate amounts of drug, nanogels or polymeric conjugates were added. Samples were incubated in full medium for 72 h at 37 °C, and the metabolic activity of each sample was determined by adding 20 μL of a 5 mg/mL of MTT stock solution in sterile PBS buffer to each well. The samples were then incubated for 2 h at 37°C, the medium and the MTT dye were washed out by PBS, and 100 μL of extraction buffer (20% w/v SDS in DMF/water, 1:1, pH 4.7) was added to each well. Samples were incubated for 24 h at 37°C. Optical absorbance was measured at 560 nm using a Model 680 microplate reader (BioRad, Hercules, CA) and cytotoxicity was expressed as a percentage of survived cells relative to non-treated control cells. All samples were analyzed by an average of eight measurements (means ± SEM). These data were plotted versus drug/nanogel concentrations and converted into IC_{50} values (concentration of the 50% cell survival).

In vivo tumor growth inhibition assay

These experiments were performed using female nu/nu mice (RL7/G cells) or male nu/nu mice (PC-3 cells), aged 6–8 weeks (Charles River Laboratories, Wilmington, MA). Animal studies were carried out according to the Principles of Animal Care outlined by the National Institutes of Health, and protocols were approved by the Institutional Animal Care and Use Committee at the University of Nebraska Medical Center. The animals were randomly divided into groups of five per cage and maintained under sterile conditions and 12-h light/dark cycle in a temperature-controlled environment. All manipulations with animals were performed in a sterile laminar hood using sterile solutions. PC-3 and RL7/G cell suspensions of 5×10^6 cells/400 μL of medium containing 20% Matrigel (Becton-Dickinson, San Diego, CA) were injected subcutaneously in the right flank areas of mice. After tumors could be palpitated, the treatment solutions of CPVA31-p_4FdU were injected peritumorally (2×100 μL) twice a week at a dose of 12 mg FdU/kg. Tumor volume was measured by digital calipers and calculated based on the equation: $TV=L/2 \times W^2$, where L and W are length and width of tumor (mm).

Results and Discussion

Synthesis of nanogel conjugates

Cholesterol is a well-known hydrophobic moiety used in many drug delivery applications in order to enhance the interactions of modified macromolecules or nanocarriers with the cellular membrane[26,27]. In our design of polymeric conjugates, we have exploited polymer modification with cholesterol for several reasons: (i) to render hydrophilic polymers soluble in organic solvents, (ii) to compel the modified polymers to form compact nanogels, and (iii) to increase membranotropic properties and ease transport of hydrophilic drug molecules across the cellular membrane. In aqueous solutions at ultrasonication cholesterol-modified polymers form ‘flower-type’ micelles with internally aggregated cholesterol moieties with the least association numbers 4–6[28]. We synthesized the cholesterol-modified polyvinyl alcohol (CPVA) containing six hydrophobic moieties per polymer chain by reaction of the corresponding PVA, M.w. 13 and 31 kDa, with cholesterol chloroformate in dry DMSO in the presence of triethylamine at room temperature. The cholesterol-modified PVA polymers were isolated with a yield of 80–85%. In an alternative method, PVA was modified in N-methyl pyrrolidone at 70°C, yielding the corresponding cholesterol-modified polymer at 70–75 % as a white solid after precipitation in diethyl ether[29]. The cholesterol-modified PVA polymers were designated as CPVA13 and CPVA31 (Scheme 1). Similarly, as shown in Scheme 2, we synthesized a cholesterol-modified dextrin (CDEX) with a high yield starting from dextrin (M.w. 9 kDa). Four cholesterol moieties were attached to the smaller dextrin

molecule. The flexibility of charged polymer chains was restricted by hydrophobic cholesterol groups aggregated in the core of nanogels. The nanogels bearing negative charged phosphate groups formed even smaller spherical compacted particles following the addition of positively charged spermine molecules (Figure 1).

^{1}H NMR spectra showed that the cholesterol modification was nearly quantitative and amounted for six moieties per polymer chain in CPVA13 and CPVA31 and four per polymer chain in CDex9. Similarly, the formation of micelles in aqueous solutions by these polymers was also demonstrated by ^{1}H NMR spectroscopy. Figures S1 and S2 represent the spectra of CPVA13 and CDex9 in (a) D_2O and (b) DMSO-d_6, respectively (see Supporting Materials). As shown in the spectra, proton signals of the cholesterol moiety (δ=0.6–2.4 ppm) appeared in DMSO-d_6 (b), but completely disappeared or wide broadening of signals was observed in D_2O (a). This indicates the restricted molecular motion of cholesterol moieties upon self-aggregation. Our results confirmed the formation of a rigid core of hydrophobic cholesterol moieties and a relatively mobile shell consisting of hydrophilic PVA or Dex molecules in aqueous medium. The degree of cholesterol substitution (DS) was evaluated by calculating the ratio between the integrals of the protons in terminal CH_3-groups of cholesterol and methylene protons in CPVA or the protons of sugar monomers in CDex.

The hydroxyl functional groups in the cholesterol-modified polymers have been used as sites for the conjugation of the active phosphorylated nucleoside analog, floxuridine (FdU), resulting in the formation of polymeric conjugates as anticancer drug carriers (Scheme 1 and 2). The 5′-hydroxyl group of the nucleoside analog was chemically attached via a biodegradable tetraphosphate linker to nanogels using a 2-cyanoethyl-bis(imidazolyl)phosphate, CNEtOP(O)Im_2, as a phosphorylating reagent. As shown in Scheme 1 and 2, the polymers were phosphorylated with CNEtOP(O)Im_2 in DMF and then reacted efficiently with inorganic pyrophosphate in the form of tetra-n-butylammonium salt PPi-TBA(**6**) in order to form the polymeric triphosphate **7**. Separately, the 5′-hydroxyl group of the nucleoside was phosphorylated by CNEtOP(O)Im_2, and the activated 5′-phosphorylated nucleoside **8** was reacted in the next step with the polymeric triphosphate **7**.

In our preliminary experiments, we found that a similar phosphorylating agent, methyl-bis(imidazolyl)phosphate, MeOPOIm_2, reacted efficiently with the primary hydroxyl groups of nucleosides in the formation of activated 5′-monophosphates, but compared with CNEtOP(O)Im_2, this reaction was much slower. The relative efficacy of phosphorylation using these two reagents was compared based on the yields of nucleoside 5′-monophosphate analyzed by ion-pair HPLC. During the first hour of reaction, CNEtOP(O)Im_2 yielded 80% of monophosphate compared with only 10% when MeOPOIm_2 was used.. The electron donor effect of the methoxy group makes the phosphorous atom less electrophilic, which resulted in longer reaction times, especially with secondary hydroxyl groups. However, both phosphorylating agents formed the same final activated 5′-monophosphorylated nucleoside in our synthesis. Next, the activated imidazolyl-phosphate moiety **8** readily reacted with polymer-triphosphate **7** and converted into nucleoside 5′-tetraphosphate anchored to CPVA, (**9–11**) or CDex (**14, 15**). Initially, we used thymidine (T) as a model drug in this study. Polymeric conjugates were purified by extensive dialysis to remove all reactants. CPVA- and CDex-conjugated 5′-tetraphosphates of FdU were designated as CPVA13-p_4FdU, CPVA31-p_4FdU, CDex9-p_4FdU and CDex9-p_4T and their properties are shown in Table 1. The amount of nucleoside attached to the polymer was determined by UV absorbance. We observed a high degree of nucleoside loading in nanogels, which was equal to 0.4–0.5 μmol/mg.

Covalent conjugation of the nucleoside to nanogels via a tetraphosphate linker was further verified by ^{31}P-NMR and IR spectroscopy. ^{31}P-NMR spectra confirmed the formation of tetraphosphate structures along with trace amounts of a triphosphate and polyphosphates such as a pentaphosphate (Figure 2). According to published chemical shifts[30,31], upper field region of ^{31}P-NMR spectra at −20 to −25 ppm corresponds to β- and γ-phosphates (peaks *c, d* and *e*), while signals between −8 to −12 ppm correspond to terminal α- and δ-phosphates (peaks *a* and *b*). IR spectra of CPVA-p_4FdU have allowed us to observe conjugation of the FdU nucleoside to the CPVA nanogel (Figure S3). As is clearly shown in the spectra, the peak at 899 cm^{-1} corresponding to P-OR stretch, the peak at 1234 cm^{-1} corresponding to P=O stretch of phosphate, and the peak at 1708 cm^{-1} corresponding to C=O stretch of amide are clearly increased in the CPVA-p_4FdU products, while peaks at 1311–1417 cm^{-1} corresponding to O-H bonding of CPVA were reduced, confirming the formation of a polyphosphate linker between CPVA and FdU.

Particle size and zeta-potential

Compact nanogel conjugates could be successfully formed as the result of self-organization of CPVA/CDex-p_4FdU molecules during ultrasonication in aqueous solutions. When sufficient energy was applied, the cholesterol moieties formed compact intramolecular clusters surrounded by a hydrophilic polymeric shell containing the embedded negatively-charged drug molecules. The particle size, homogeneity, and morphology of CPVA/CDex-p_4FdU structures were measured by dynamic light scattering (DLS) and transmission electron microscopy (TEM). A single sharp peak in DLS profiles with a hydrodynamic diameter in the range of 12–45 nm implied the presence of a single population of small particles with a relatively low polydispersity index of 0.30–0.59 (Table 1). The high negative zeta- potential of CPVA/CDex-p_4FdU confirmed the presence of phosphates in the surface layer of polymeric conjugates. TEM pictures showed the spherical particle morphology with hydrodynamic diameters in the range of 38–58 nm (Figure 3). We have also studied the change in particle size after neutralization of the negative charge in polymeric conjugates with the polyamine spermine (Figure 1). The addition of positively-charged spermine at physiological conditions resulted in a 2–3-fold reduction in hydrodynamic and TEM-observed diameters and the change in morphology of particles, e.g. the appearance of a thicker electron-dense exterior layer surrounding these compacted polymeric conjugates[32].

Enzymatic hydrolysis

The formation of natural nucleoside 5′-phosphate bonds between nucleoside and nanogel backbone was further confirmed using enzymatic hydrolysis by snake venom phosphodiesterase I (VPDE). VPDE was able to catalyze the hydrolysis of esterified nucleoside 5′-phosphates into a nucleoside 5′-phosphate and also the cleavage of nucleoside 5′-phosphate from oligonucleotides with a free 3′-end[33,34]. This property of VPDE allows us to investigate the enzymatic stability of nanogel-bound nucleoside phosphates. Nanogels CPVA-p_4FdU and CDex-p_4FdU were incubated with VPDE at 37 °C and then analyzed by ion-pair HPLC (Figure 4). We observed the gradual disappearance of the initial wide peak with the elution time of 25–34 min (*a*) and the formation of a sharp peak at the elution time of ca. 5 min (*b*), which corresponded to control nucleoside 5′-phosphates (TMP or FdUMP). Structure of the released nucleoside products was further confirmed by comparison of UV spectra with initial nucleoside analogs. Our data demonstrated a nearly quantitative enzymatic release of nucleotide 5′-phosphate from polymeric conjugates within 12 to 24 h.

In vitro drug release

The *in vitro* release of FdU was monitored at 37 °C at different pH values (1.0, 4.0 and 7.4) in order to assess the stability of nanogel conjugates in the environments inside of the

stomach, endosomal vesicles, and blood, respectively. Each nanogel, CPVA-p_4FdU or CDEX-p_4FdU, was placed into the appropriate buffer solution and incubated at 37 °C. Serial aliquots were removed at the appropriate times during hydrolysis, and the cleaved nucleoside/nucleotide was separated by ultrafiltration and quantified by UV absorbance. The release profiles at different pH values are shown in Figure 5. In general, polymeric conjugates displayed linear first-order reaction kinetics of hydrolysis with slower drug release at pH 7.4 and pH 4.0 than at pH 1.0. At pH 4.0 and 7.4, drug release was 1–2% per day, while at pH 1.0 drug release reached 4% per day. These results are consistent with the pH-dependent degradation behavior of other dinucleoside polyphosphates, such as diadenosine-P**1**,P**3**-triphosphate and P**1**,P**4**-tetraphosphate[35]. However, CPVA/CDex-p_4FdU conjugates showed much slower drug release compared to diadenosine-P**1**,P**4**-tetraphosphate (25 days vs. 3 days). The pH-dependent hydrolysis can be facilitated by a hydronium ion through the nucleophilic attack of protonated phosphate groups at lower pH, which results in an S_N(P) type substitution, and then the formation of a penta-coordinated phosphorus transition state and nucleoside 5′-phosphates as final products (Scheme 3). Highly hydrated polymer coils surrounding the tetraphosphate linkers evidently create a steric hindrance and significantly slow down the process.

Evidently, the release of phosphorylated nucleosides in cancer cells would provide a strong therapeutic advantage to these polymeric conjugates, because the drug component doesn't have to pass through the phosphorylation step, which is known to be a rate-limiting step in biological activation of nucleoside analogs[36]. Our data show that this type of polymeric conjugates is capable of the sustained drug release during the extended period of time and can serve as active drug depot, significantly enhancing therapeutic effect against cancer cells. Peritumoral injections or systemic administration of polymeric conjugates would result in only minimal initial drug burst, a shortcoming of many drug delivery systems at systemic administration. Additionally, accumulation of nanocarriers from blood circulation through the enhanced permeability and retention (EPR) effect in leaking tumor neovasculature can potentially enhance the tumor growth inhibitory effect. Polymeric conjugates can also be considered as potential oral therapeutic formulations due to the observed slow drug release at low pH in the digestive tract (*in vivo* experiments are underway). We have also demonstrated that enzymatic hydrolysis of polymeric conjugates is at least 20–25 times faster than hydrolytic hydrolysis. Therefore, these polymeric conjugates, which have a slow sustained drug release in tumor tissue and other organs in normal conditions *in vivo*, might be quickly activated by enzymatic activities present in the cytosol or subcellular compartments of proliferating cancer cells[37]. The most common type of hydrolytic enzymes in mammalian cells are cytosolic phosphodiesterases and nucleotide phosphatases, which can release active 5′-nucleotides from the polymeric conjugates[38].

Cytotoxicity Assay

Drug resistance to nucleoside analogs is known to be an important clinical problem in the treatment of cancer. Therapeutic effects can be achieved with nucleoside analogs as a single agent or in combination with other drugs only at the increasingly higher dosage. Here, we have studied the cytotoxicity of several polymeric conjugates of activated analogs of 5-fluorouracyl as a model drug in various cancer cell lines including ones that are resistant to nucleoside analogs. The cytotoxicity of polymeric floxuridine conjugates CPVA13-p_4FdU, CPVA31-p_4FdU and CDEX9-p_4FdU was determined in human prostate adenocarcinoma PC-3, breast carcinoma MCF-7 and MDA-MB-231, hepatic carcinoma HepG2, gemcitabine-resistant follicular lymphoma RL7/G and cytarabine-resistant T-lymphoma CEM/araC/8 cells using a thiazolyl blue (MTT) dye reduction assay[39]. As shown in Figure 6 and Table 2, nanoconjugates showed considerably enhanced cytotoxicity and lower IC_{50} values (drug concentration resulting in 50% cell death) compared to free floxuridine in all of

these cell lines. The enhancement factor (EF), which is equal to IC_{50}(drug)/IC_{50}(conjugate), was used as a measure of the increase in cytotoxicity of polymeric conjugates compared to free drug. Nanogels without conjugated drug demonstrated no cytotoxicity (IC_{50} > 10 mg/mL). All of these polymeric conjugates showed a higher EF in drug resistant cell lines, CEM/araC/8 and RL7/G, compared to other tumor cells. Specifically, CPVA13-p_4FdU and CDex9-p_4FdU exhibited an EF of 100 and 85 in CEM/araC/8 cells, while the EF showed by other cells was normally in the lower range of 3.5–50.

In vivo tumor growth inhibition

The therapeutic efficacy of polymeric conjugates was evaluated in subcutaneous (*s.c.*) human prostate adenocarcinoma PC-3 and gemcitabine-resistant follicular lymphoma RL7/G tumor xenograft mouse models. These tumors were established by *s.c.* injection of tumor cells in the lower flank areas of athymic *nu–nu* mice. After the observation of the initial tumors, animals were randomly separated into control and treatment groups (n = 5–6). Median tumor volume was measured by digital calipers twice a week simultaneously with peritumoral injections of polymeric conjugates with a dose of 80 mg/kg, which is equivalent to 10 mg FdU/kg. This way of administration allowed a subcutaneous storage of the viscous polymer-drug conjugate and the sustained release of activated drug into the tumor. We observed a strong 6.5-fold tumor growth inhibition in human prostate carcinoma PC-3 model that confirms the high therapeutic potential of polymeric conjugates (Figure 7A). Although the observed 2-fold growth inhibition was lower in drug-resistant human follicular lymphoma RL7/G tumors compared to PC-3 tumors, the effect of the CPVA31-p_4FdU conjugate was statistically significant ($P < 0.05$) (Figure 7B). The significance of the experimental data was determined by a two tailed Student's *t*-test. No significant weight loss or acute toxicity of polymeric conjugates was observed during the entire period of treatment. Tumors removed from experimental animals at the end of the experiments were clearly smaller than tumors in the control group (Figure 7C).

Conclusions

We have developed a novel type of covalently-bound polymeric phosphorylated nucleoside analogs, polymeric conjugates, for a sustained delivery of the activated anticancer drugs into tumors. These carriers combine attractive properties of biocompatible polymers with an enhanced cytotoxic efficacy of activated nucleoside analogs and form compact drug-loaded polymeric nanoparticles. *In vitro* evaluation against various cancer cell lines, including drug-resistant cancer cells, demonstrated that the activated floxuridine conjugate has 50–100 times stronger cytotoxicity compared to free nucleoside analog. Furthermore, the observed sustained drug release was a potential cause of the increased tumor growth inhibition following the peritumoral administration of polymeric conjugates in subcutaneous tumor xenograft models. This class of anticancer drug formulations also has features, which makes them a very promising vehicle for oral administration of activated phosphorylated nucleoside analogs.

Supplementary Material

Refer to Web version on PubMed Central for supplementary material.

Acknowledgments

The financial support from National Cancer Institute (R01 CA136921 for S.V.V.) is gratefully acknowledged. The authors thank Tom Bargar of the Electron Microscopy Core Facility, Ed Ezell of the NMR Core Facility and Marina Sokolsky-Papkov from Center for Drug Delivery and Nanomedicine (University of Nebraska Medical Center) for providing assistance with TEM microscopy, NMR and IR spectroscopy, respectively. We are grateful to Trevor Gerson for his help in the revision of the manuscript.

References

1. Johnstone RW, Ruefli AA, Lowe SW. Apoptosis: a link between cancer genetics and chemotherapy. Cell. 2002; 108:153–164. [PubMed: 11832206]
2. Galmarini CM, Mackey JR, Dumontet C. Nucleoside analogues and nucleobases in cancer treatment. Lancet Oncol. 2002; 3:415–424. [PubMed: 12142171]
3. Galmarini CM, Thomas X, Calvo F, Rousselot P, Rabilloud M, El Jaffari A, Cros E, Dumontet C. In vivo mechanisms of resistance to cytarabine in acute myeloid leukaemia. Br J Haematol. 2002; 117:860–868. [PubMed: 12060121]
4. Ward JL, Sherali A, Mo ZP, Tse CM. Kinetic and pharmacological properties of cloned human equilibrative nucleoside transporters, ENT1 and ENT2, stably expressed in nucleoside transporter-deficient PK15 cells. Ent2 exhibits a low affinity for guanosine and cytidine but a high affinity for inosine. J Biol Chem. 2000; 275:8375–8381. [PubMed: 10722669]
5. Crawford CR, Ng CY, Belt JA. Isolation and characterization of an L1210 cell line retaining the sodium-dependent carrier cif as its sole nucleoside transport activity. J Biol Chem. 1990; 265:13730–13734. [PubMed: 1974252]
6. Crawford CR, Ng CY, Noel LD, Belt JA. Nucleoside transport in L1210 murine leukemia cells. Evidence for three transporters. J Biol Chem. 1990; 265:9732–9736. [PubMed: 2351668]
7. Funato T, Satou J, Nishiyama Y, Fujimaki S, Miura T, Kaku M, Sasaki T. In vitro leukemia cell models of Ara-C resistance. Leuk Res. 2000; 24:535–541. [PubMed: 10781689]
8. Dumontet C, Fabianowska-Majewska K, Mantincic D, Callet Bauchu E, Tigaud I, Gandhi V, Lepoivre M, Peters GJ, Rolland MO, Wyczechowska D, Fang X, Gazzo S, Voorn DA, Vanier-Viornery A, MacKey J. Common resistance mechanisms to deoxynucleoside analogues in variants of the human erythroleukaemic line K562. Br J Haematol. 1999; 106:78–85. [PubMed: 10444166]
9. Meier C, Balzarini J. Application of the cycloSal-prodrug approach for improving the biological potential of phosphorylated biomolecules. Antiviral Res. 2006; 71:282–292. [PubMed: 16735066]
10. Galmarini CM, Popowycz F, Joseph B. Cytotoxic nucleoside analogues: different strategies to improve their clinical efficacy. Curr Med Chem. 2008; 15:1072–1082. [PubMed: 18473803]
11. Zamboni WC. Liposomal, nanoparticle, and conjugated formulations of anticancer agents. Clin Cancer Res. 2005; 11:8230–8234. [PubMed: 16322279]
12. Crosasso P, Brusa P, Dosio F, Arpicco S, Pacchioni D, Schuber F, Cattel L. Antitumoral activity of liposomes and immunoliposomes containing 5-fluorouridine prodrugs. J Pharm Sci. 1997; 86:832–839. [PubMed: 9232525]
13. Duzgunes N, Simoes S, Slepushkin V, Pretzer E, Flasher D, Salem, Steffan G, Konopka K, Pedroso de Lima MC. Delivery of antiviral agents in liposomes. Methods Enzymol. 2005; 391:351–373. [PubMed: 15721391]
14. Oussoren C, Magnani M, Fraternale A, Casabianca A, Chiarantini L, Ingebrigsten R, Underberg WJ, Storm G. Liposomes as carriers of the antiretroviral agent dideoxycytidine-5′-triphosphate. Int J Pharm. 1999; 180:261–270. [PubMed: 10370196]
15. Vinogradov SV, Poluektova LY, Makarov E, Gerson T, Senanayake MT. Nano-NRTIs: efficient inhibitors of HIV type-1 in macrophages with a reduced mitochondrial toxicity. Antivir Chem Chemother. 2010; 21:1–14. [PubMed: 21045256]
16. Magnani M, Rossi L, Fraternale A, Casabianca A, Brandi G, Benatti U, De Flora A. Targeting antiviral nucleotide analogues to macrophages. J Leukoc Biol. 1997; 62:133–137. [PubMed: 9226004]
17. Vinogradov SV, Zeman AD, Batrakova EV, Kabanov AV. Polyplex Nanogel formulations for drug delivery of cytotoxic nucleoside analogs. J Control Release. 2005; 107:143–157. [PubMed: 16039001]
18. Vinogradov SV, Kohli E, Zeman AD. Cross-linked polymeric nanogel formulations of 5′-triphosphates of nucleoside analogues: role of the cellular membrane in drug release. Mol Pharm. 2005; 2:449–461. [PubMed: 16323952]
19. Galmarini CM, Warren G, Kohli E, Zeman A, Mitin A, Vinogradov SV. Polymeric nanogels containing the triphosphate form of cytotoxic nucleoside analogues show antitumor activity

against breast and colorectal cancer cell lines. Mol Cancer Ther. 2008; 7:3373–3380. [PubMed: 18852140]

20. Aryal S, Hu CM, Zhang L. Combinatorial drug conjugation enables nanoparticle dual-drug delivery. Small. 2010; 6:1442–1448. [PubMed: 20564488]
21. Ferey G. Hybrid porous solids: past, present, future. Chem Soc Rev. 2008; 37:191–214. [PubMed: 18197340]
22. Ulbrich K, Strohalm J, Kopecek J. Polymers containing enzymatically degradable bonds. VI. Hydrophilic gels cleavable by chymotrypsin. Biomaterials. 1982; 3:150–154. [PubMed: 7115858]
23. Galmarini CM, Clarke ML, Jordheim L, Santos CL, Cros E, Mackey JR, Dumontet C. Resistance to gemcitabine in a human follicular lymphoma cell line is due to partial deletion of the deoxycytidine kinase gene. BMC Pharmacol. 2004; 4:8. [PubMed: 15157282]
24. Ullman B. Dideoxycytidine metabolism in wild type and mutant CEM cells deficient in nucleoside transport or deoxycytidine kinase. Adv Exp Med Biol. 1989; 253B:415–420. [PubMed: 2558543]
25. Sinha ND, Biernat J, McManus J, Koster H. Polymer support oligonucleotide synthesis XVIII: use of beta-cyanoethyl-N,N-dialkylamino-/N-morpholino phosphoramidite of deoxynucleosides for the synthesis of DNA fragments simplifying deprotection and isolation of the final product. Nucleic Acids Res. 1984; 12:4539–4557. [PubMed: 6547529]
26. Vinogradov SV, Suzdaltseva Y, Alakhov V, Kabanov AV. Inhibition of herpes simplex virus 1 reproduction with hydrophobized antisense oligonucleotides. Biochem Biophys Res Commun. 1994; 203:959–966. [PubMed: 8093080]
27. Nochi T, Yuki Y, Takahashi H, Sawada S, Mejima M, Kohda T, Harada N, Kong IG, Sato A, Kataoka N, Tokuhara D, Kurokawa S, Takahashi Y, Tsukada H, Kozaki S, Akiyoshi K, Kiyono H. Nanogel antigenic protein-delivery system for adjuvant-free intranasal vaccines. Nat Mater. 2010; 9:572–578. [PubMed: 20562880]
28. Yusa S, Kamachi M, Morishima Y. Hydrophobic self-association of cholesterol moieties covalently linked to polyelectrolytes: Effect of spacer bond. Langmuir. 1998; 14:6059–6067.
29. Gimenez V, Reina JA, Mantecon A, Cadiz V. Unsaturated modified poly(vinyl alcohol). Crosslinking through double bonds. Polymer. 1999; 40:2759–2767.
30. Moreno B, Urbina JA, Oldfield E, Bailey BN, Rodrigues CO, Docampo R. 31P NMR spectroscopy of Trypanosoma brucei, Trypanosoma cruzi, and Leishmania major. Evidence for high levels of condensed inorganic phosphates. J Biol Chem. 2000; 275:28356–28362. [PubMed: 10871617]
31. Warnecke S, Meier C. Synthesis of nucleoside Di- and triphosphates and dinucleoside polyphosphates with cycloSal-nucleotides. J Org Chem. 2009; 74:3024–3030. [PubMed: 19320463]
32. Chen N, Murata S, Yoshikawa K. Dramatic change in the tertiary structure of giant DNA without distortion of the secondary structure caused by pteridine-polyamine conjugates. Chemistry. 2005; 11:4835–4840. [PubMed: 15954150]
33. Razzell WE, Khorana HG. Studies on polynucleotides. III. Enzymic degradation; substrate specificity and properties of snake venom phosphodiesterase. J Biol Chem. 1959; 234:2105–2113. [PubMed: 13673021]
34. Garcia-Diaz M, Avalos M, Cameselle JC. Methanol esterification reactions catalyzed by snake venom and bovine intestinal 5′-nucleotide phosphodiesterases. Formation of nucleoside 5′-monophosphate methyl esters from guanosine 5′-triphosphate and other nucleoside 5′-polyphosphates. Eur J Biochem. 1991; 196:451–457. [PubMed: 1848820]
35. Mikkola S. Hydrolytic reactions of diadenosine 5′,5′-triphosphate. Org Biomol Chem. 2004; 2:770–776. [PubMed: 14985817]
36. Longley DB, Harkin DP, Johnston PG. 5-fluorouracil: mechanisms of action and clinical strategies. Nat Rev Cancer. 2003; 3:330–338. [PubMed: 12724731]
37. Bender AT, Beavo JA. Cyclic nucleotide phosphodiesterases: molecular regulation to clinical use. Pharmacol Rev. 2006; 58:488–520. [PubMed: 16968949]
38. Garcia-Diaz M, Avalos M, Cameselle JC. Methanol esterification reaction catalyzed by snake venom and bovine intestinal 5′-nucleotide phosphodiesterases. Eur J Biochem. 2006; 196:451–457. [PubMed: 1848820]

39. Hansen MB, Nielsen SE, Berg K. Re-examination and further development of a precise and rapid dye method for measuring cell growth/cell kill. J Immunol Methods. 1989; 119:203–210. [PubMed: 2470825]

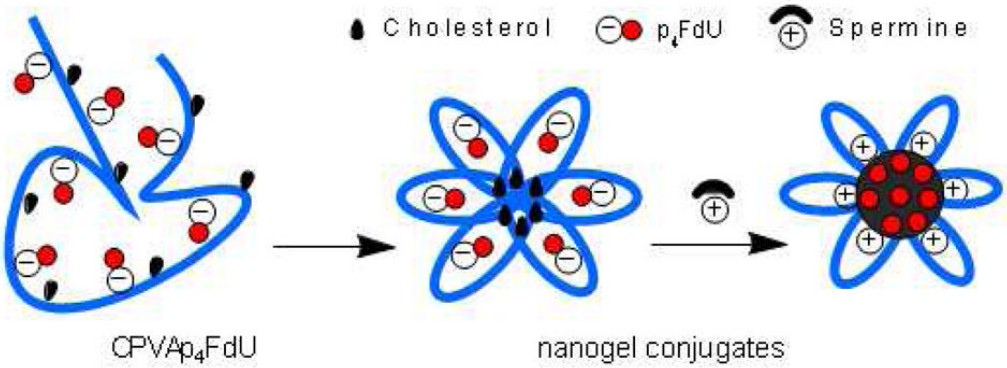

Figure 1.
Formation of compact nanogels from polymer drug conjugates

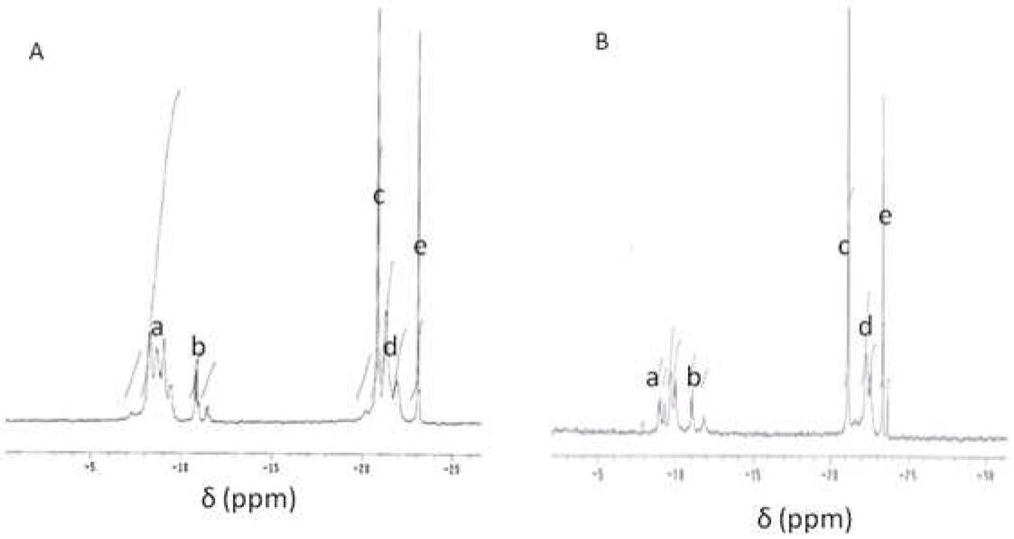

Figure 2.
31P-NMR spectrum of polymeric conjugates, CPVA31-p_4FdU (A) and CDex9-p4FdU (B) (phosphorus signals a-e are described in the text)

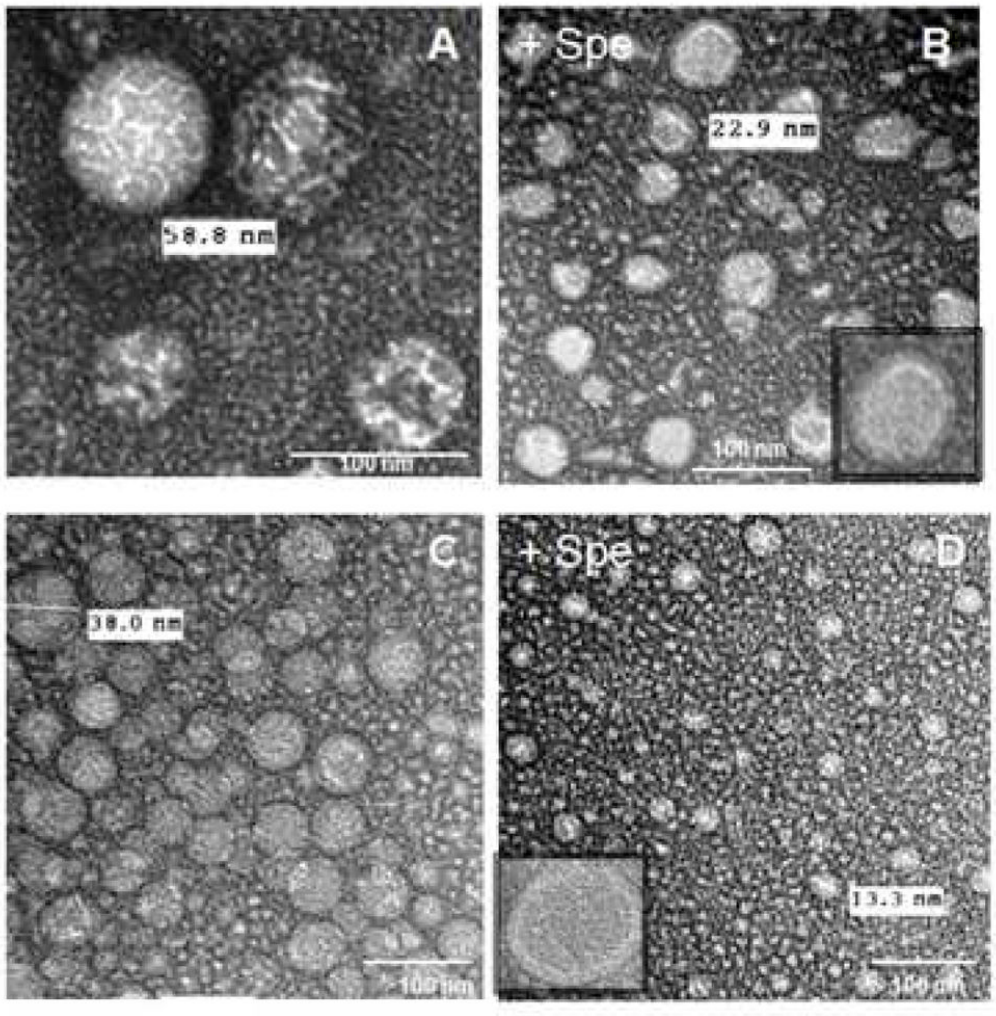

Figure 3.
Transmission electron microscopy (TEM) images of nanogels formed from polymer conjugates: (A) CPVA31-p_4FdU, (B) its spermine complex (Spe), (C) CDex9-p_4FdU, and (D) its spermine complex. Samples were stained with vanadate.

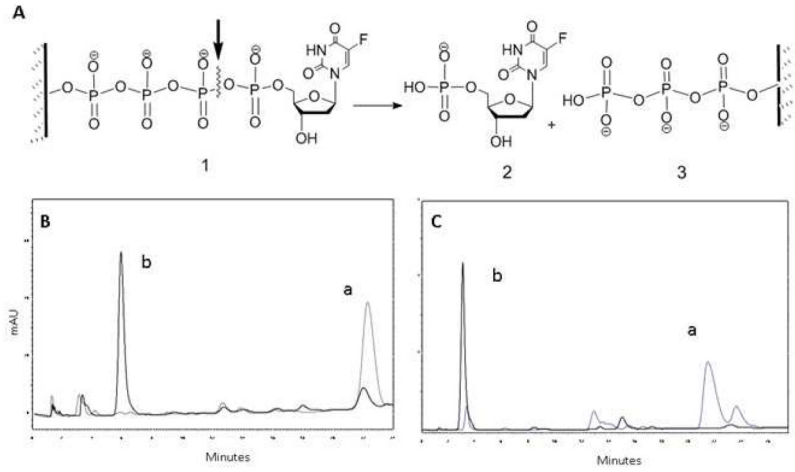

Figure 4.

Enzymatic hydrolysis of polymeric conjugates by snake venom phosphodiesterase I (VPDE). (A) The enzyme hydrolyzes the P-O bond at α-phosphate group in nanogel conjugate resulting in nucleoside 5′-phosphate (2). (B) Ion-pair HPLC profiles of initial (a) and hydrolyzed (b) CPVA31-p_4FdU. (C) Ion-pair HPLC profiles of initial (a) and hydrolyzed (b) CDex9-p_4T after 24 h-incubation with 0.01 units of VPDE enzyme.

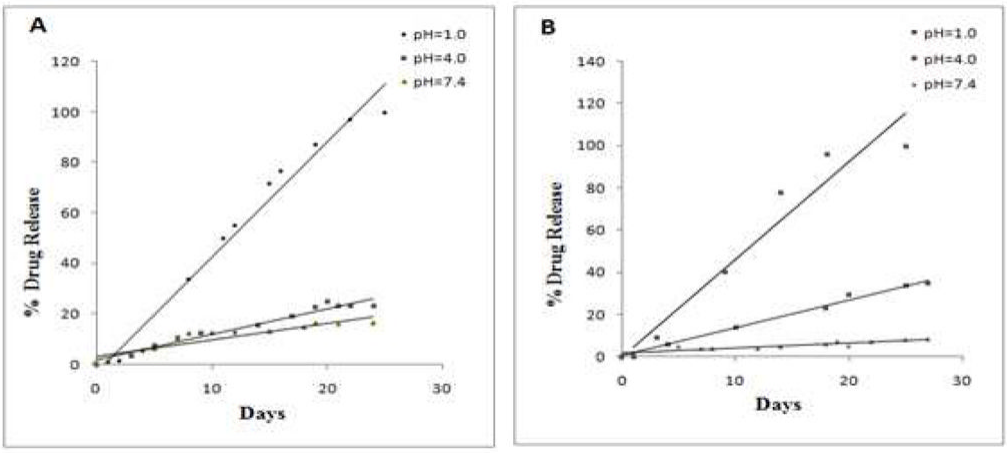

Figure 5.
In vitro drug release from polymeric conjugates CPVA31-p_4FdU (A) and CDex9-p_4FdU (B) at different pH in buffered saline.

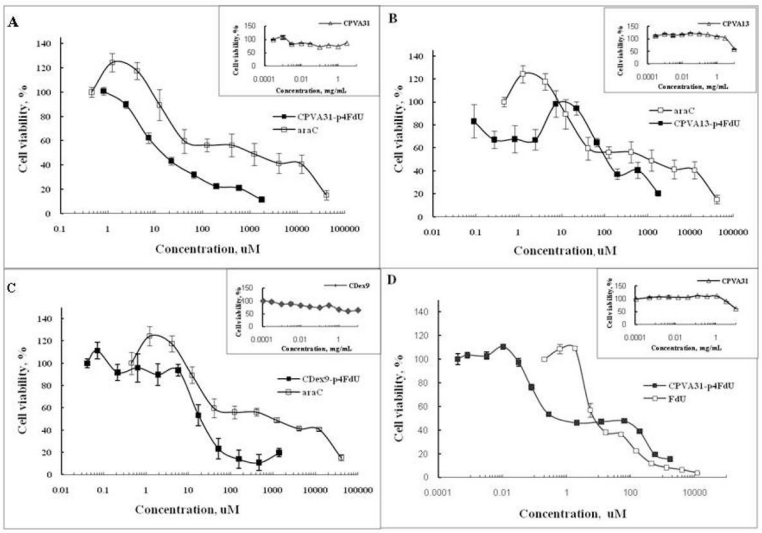

Figure 6.

Cytotoxicity of polymeric conjugates in drug-resistant human T-lymphoma CEM/araC/8 cells (A–C) and prostate carcinoma PC-3 cells (D).

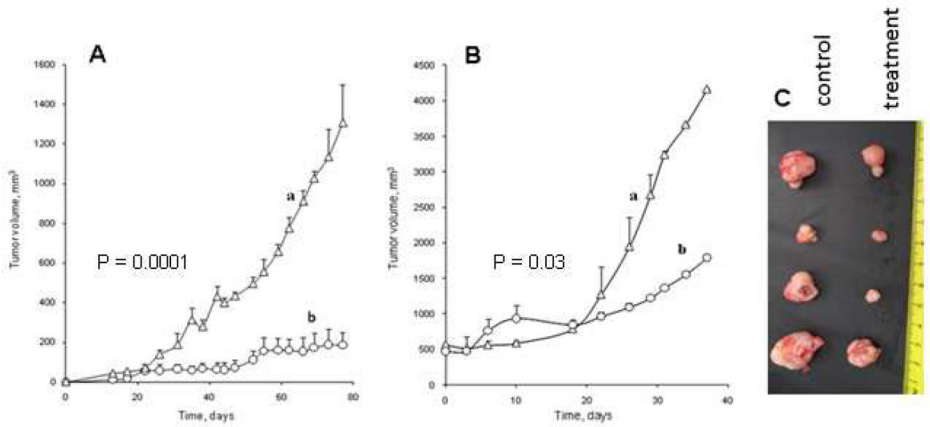

Figure 7.

Tumor growth inhibition in mice with subcutaneous human prostate carcinoma PC-3 (A) and gemcitabine-resistant follicular lymphoma RL7/G (B) tumors following the peritumoral injections of the polymeric conjugate CPVA31-p4FdU (dose 80 mg/kg, or 10 mg FdU/kg). The data were statistically significant with $P<0.05$ between (a) control and (b) treatment groups. (C) Tumor photographs in the end of the experiment B taken from control and treatment groups.

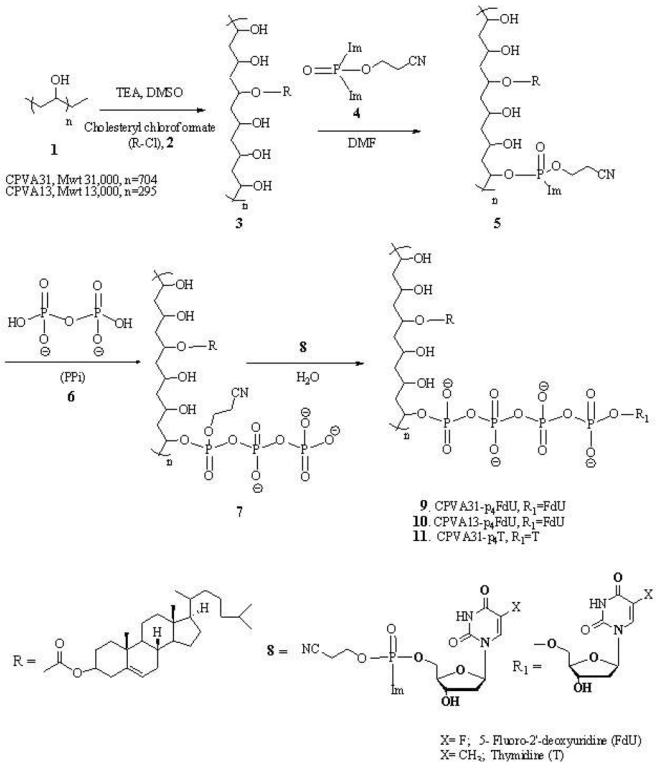

Scheme 1.
Synthetic steps in the preparation of CPVA conjugates

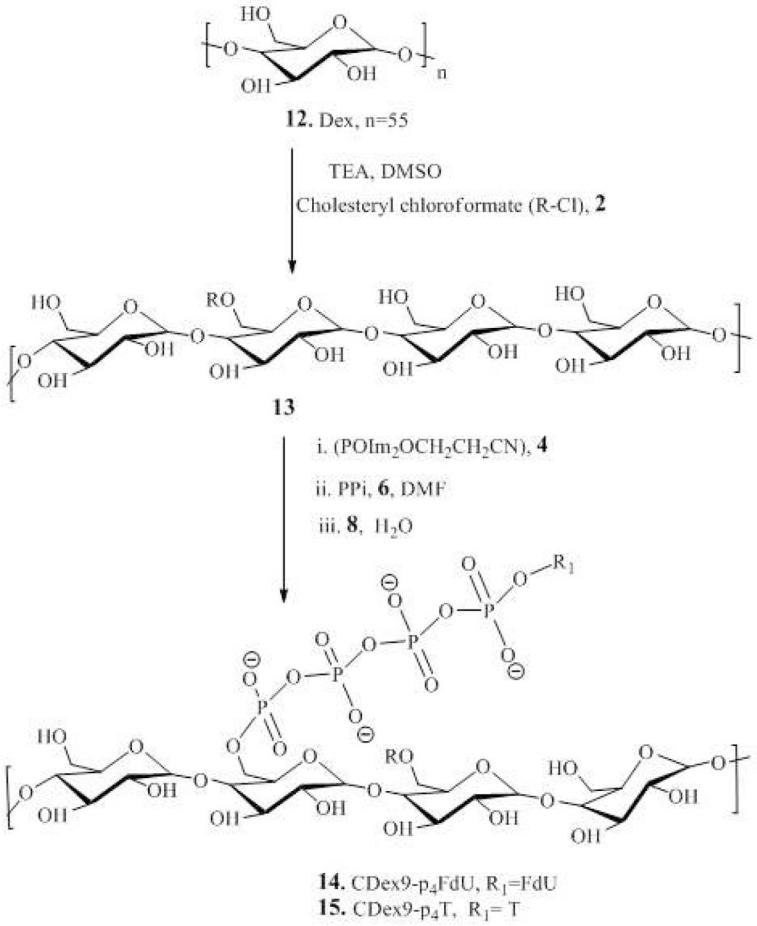

Scheme 2.
Synthesis of CDex-conjugates (compounds 1–11, see Scheme 1).

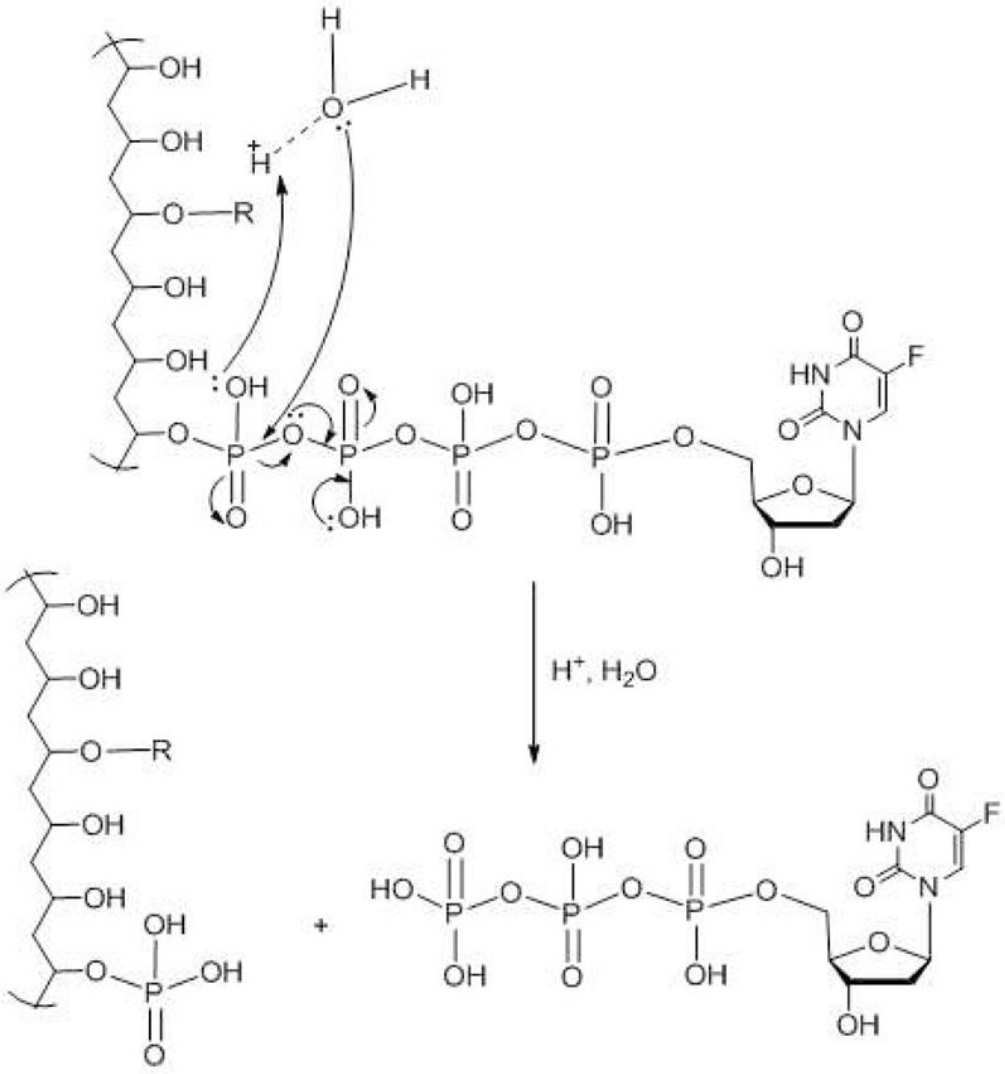

Scheme 3.
Mechanism of acidic hydrolysis of polymeric conjugates and release of phosphorylated nucleosides (R = cholesterol).

Table 1

Particle characteristics of polymeric conjugates

Polymeric conjugate*	d_h, nm (volume- averaged)	PDI	ζ, mV
CPVA31	35.00 ± 1.30	0.361 ± 0.01	0.00 ± 3.70
CPVA31-p_4FdU	42.12 ± 6.41	0.405 ± 0.04	−8.47 ± 3.60
CPVA13	12.52 ± 5.12	0.596 ± 0.03	−2.57 ± 3.40
CPVA13-p_4FdU	34.95 ± 5.43	0.417 ± 0.01	−34.0 ± 4.67
CDEX9	44.53 ± 8.34	0.458 ± 0.02	−8.00 ± 4.02
CDEX9-p_4FdU	26.23 ± 4.12	0.440 ± 0.03	−34.80 ± 5.06
CDEX9-p_4T	18.27 ± 2.01	0.508 ± 0.00	0.00 ± 4.52

* Particle size (d_h), polydispersity index (PDI) and zeta potential (ζ) were measured in 1% solutions in water after 2 h-sonication. The results are average values ± SD of three measurements.

Table 2

Cytotoxicity of cytotoxic drugs, polymeric conjugates and drug conjugates in cancer cells

	IC_{50} values (μM)*					
Drug formulation	**PC-3**	**MCF-7**	**HepG2**	**MDA-MB-231**	**CEM/araC/8**	**RL7/G**
Floxuridine (FdU)	6.5	12195	2195	14.2		
Cytarabine (araC)					1234	
Gemcitabine (G)						19011
CPVA31	>10	>10	>10	>10	>10	>10
CPVA13	>10	>10	>10	>10	>10	>10
CDEX9					>10	>10
CPVA31-p_4FdU	0.4 (EF=16)	2032 (EF=6)	487 (EF=4.5)	0.28 (EF=50)	12.3 (EF=100)	3802 (EF=5)
CPVA13-p_4FdU	81.3	813 (EF=15)	609.7 (EF=3.6)	0.6 (EF=23)	102 (EF=12)	950 (EF=20)
CDEX9-p_4FdU					14.5 (EF=85)	

*Cytotoxicity was measured after 72-h treatment. IC_{50} of CPVA31, CPVA13 and CDEX9 in each cell line are given in mg/mL. EF = enhancement factor showing the efficacy compared to free drug.